Supporting Information for:

Measurement report: Fast photochemical production of peroxyacetyl nitrate (PAN) over the rural North China Plain during cold-season haze events

Yulu Qiu[1,2,3,4], Zhiqiang Ma[1,3,4,*], Ke Li[5], Mengyu Huang[6], Jiujiang Sheng[6], Ping Tian[6], Jia Zhu[2], Weiwei Pu[3,4], Yingxiao Tang[7], Tingting Han[3,4], Huaigang Zhou[3,4], and Hong Liao[2]

[1]Institute of Urban Meteorology, China Meteorological Administration, Beijing, 100089, China

[2]Collaborative Innovation Center of Atmospheric Environment and Equipment Technology, Jiangsu Key Laboratory of Atmospheric Environment Monitoring and Pollution Control (AEMPC), School of Environmental Science and Engineering, Nanjing University of Information Science & Technology, Nanjing, 210044, China

[3]Beijing Shangdianzi Regional Atmosphere Watch Station, Beijing, 101507, China

[4]Environmental Meteorology Forecast Center of Beijing-Tianjin-Hebei, Beijing, 100089, China

[5]John A. Paulson School of Engineering and Applied Sciences, Harvard University, Cambridge, MA 02138, USA

[6]Beijing Weather Modification Office, Beijing, 100089, China

[7]Tianjin Environmental Meteorology Center, Tianjin, 300074, China

Correspondence to: Zhiqiang Ma (zqma@ium.cn)

Contents:

Method S1. Calculation of physical impacts and local chemical formation of PAN

Ambient PAN concentration is affected by physical processes (such as regional transport) and local photochemical formation. Here, we define that the transport impacts are restricted to PAN itself, exclusive of PAN's precursors. Thus, the change rate of PAN concentration ($\frac{d[PAN]}{dt}$) is the sum of net chemical production ($\frac{d[Chem]}{dt}$) and physical changes ($\frac{d[Phys]}{dt}$) as shown in Eq.1. The ratio of changes in PAN concentration due to physical processes to the base concentration is assumed to be identical with the change ratio of CO (Eq.2), as CO is usually considered as a chemically inert species and also abundant in the urban region. The net chemical production of PAN is a combined result of chemical production (P[PAN]) and thermal decomposition (L[PAN], Eq.3). PAN's thermal decomposition can be directly derived (Eq.4) and the chemical reaction rate coefficient *k* is temperature-dependent and obtained from Seinfeld and Pandis (2006). The chemical production of PAN (P[PAN]) can be obtained from the difference between net chemical production rate and chemical loss rate (Eq.5). In this study, we use 4 hours as dt and sperate a day as morning (8:00−12:00), afternoon (12:00−16:00), evening (16:00−20:00) and night (20:00−08:00).

$$\frac{d[PAN]}{dt} = \frac{d[Chem]}{dt} + \frac{d[Phys]}{dt} \quad \text{(Eq.1)}$$

$$\frac{d[Phys]}{dt} = \frac{d[CO]}{dt} \times \frac{[PAN]}{[CO]} \quad \text{(Eq.2)}$$

$$\frac{d[Chem]}{dt} = \frac{d[PAN]}{dt} - \frac{d[CO]}{dt} \times \frac{[PAN]}{[CO]} = P[Chem] + L[Chem] \quad \text{(Eq.3)}$$

$$L[Chem] = -k[PAN] \quad \text{(Eq.4)}$$

$$P[Chem] = \frac{d[PAN]}{dt} - \frac{d[CO]}{dt} \times \frac{[PAN]}{[CO]} + k[PAN] \quad \text{(Eq.5)}$$

Method S2. Calculation of HO_x production rates through three pathways

Photolysis of O_3, HONO and HCHO are usually considered as the three major HO_x sources. Photolysis of HONO can directly produce OH radical (R1) and its production rate of HO_x ($P[HO_x]_{HONO}$) is the product of photolysis rate and HONO concentration (Eq. 6). O_3 photolysis can produce excited singlet oxygen atom ($O(^1D)$, R2), and $O(^1D)$ collides with N_2 or O_2, quenching to its ground state (R3) or reacts with H_2O to generate two OH radicals (R4). Following the estimation method in Seinfeld and Pandis (2006), the HO_x production rate by O_3 photolysis could be derived in Eq. 7. Photolysis of HCHO directly produces H and HCO. Because of the rapid reaction between HCO (H) and O_2, HCHO photolysis could be represented in R5, and the production rate of HO_x is calculated following Eq. 8.

$$HONO + hv \rightarrow OH + NO \quad \text{(R1)}$$

$$P[HOx]_{HONO} = J(HONO) \times [HONO] \quad \text{(Eq.6)}$$

$$O_3 + hv \rightarrow O(^1D) + O_2 \quad \text{(R2)}$$

$$O(^1D) + [M] \rightarrow O + M \quad \text{(R3)}$$

$$O(^1D) + H_2O \rightarrow 2OH \quad \text{(R4)}$$

$$P[HOx]_{O_3} = \frac{2J(O_3) \times k_4 \times [H_2O] \times [O_3]}{[M] \times k_3} \quad \text{(Eq.7)}$$

$$HCHO + hv + 2O_2 \rightarrow 2HO_2 + CO \quad \text{(R5)}$$

$$P[HOx]_{HCHO} = 2J[HCHO] \times [HCHO] \quad \text{(Eq.8)}$$

Table S1. Detailed parameters of instruments used in this study.

Species	Instruments	Time resolution	Detection limit	Calibration frequency
PAN	GC-ECD	5 min	20 pptv	monthly
VOCs	PTR-ToF-MS	5 min	-	quarterly
HONO	LOPAP	1 min	10 pptv	weekly
O_3	TE 49i	1 min	0.5 ppbv	monthly
NO_x	TE 42i	1 min	50 pptv	monthly
CO	Picarro, G2401	2 sec	40 ppbv	monthly
$PM_{2.5}$	TEOM 1405	5 min	0.1 μg/m³	-
Photolysis (*J*)	PFS-100	1 min	-	quarterly

Table S2. Comparisons of PAN levels in recent studies in China with results in this study.

Location	Site type	Period	Conc. (ppb)	Reference
Jinan, Shandong, China	Urban NCP	Nov 2015−Jul 2016	1.89±1.42	Liu et al. (2018)
Tianjin, China	Suburban NCP	Sep 5−28, 2018	0.93±0.57	Qiu et al. (2019a)
PKU, Beijing, China	Urban NCP	Jun−Jul, 2014	1.5	Zhang et al. (2017)
Wangdu, Hebei, China	Rural NCP	Jun−Jul, 2014	1.7	Zhang et al. (2017)
Beijing, China	Suburban NCP	Jan−Feb, 2016	1.04	Zhang et al. (2019)
CS, Chongqing, China	Urban site	Aug 25−Sep 10, 2015	2.05	Sun et al. (2020)
NQ, Chongqing, China	Suburban site	Aug 25−Sep 10, 2015	1.08	Sun et al. (2020)
Xiamen, Fujian, China	Suburban site	Jan–Dec, 2018	0.55	Hu et al. (2020)
Hongkong, China	Suburban site	Oct–Nov, 2016	0.63±0.05	Zeng et al. (2019a)
Ziyang, Sichuan, China	Urban site	Dec, 2012	0.55	Zhu et al. (2018)
Central Tibetan Plateau, China	Background site	Aug17−24, 2011	0.36	Xu et al. (2018)
		May 15−Jul 2012	0.44	
SDZ, Beijing, China	Rural NCP	Oct, 2020	1.11±0.88	This study

Table S3. Comparisons between HO_2+NO (R1) and HO_2+HO_2 (R2) during pollution days at the SDZ site.

	k[a] (cm^3 $molec^{-1}$ s^{-1})	HO_2[b] (molec cm^{-3})	NO or HO_2 (molec cm^{-3})	Production rates[c] (molec cm^{-3} s^{-1})
HO_2+NO (R1)	8.4×10^{-12}	$\sim10^8$	7.1×10^9 for NO	$\sim6\times10^6$
HO_2+HO_2 (R2)	3.3×10^{-12}	$\sim10^8$	$\sim10^8$ for HO_2	$\sim3.3\times10^4$
R1/R2	2.5	1	~71	$\sim1.8\times10^2$

[a]. *k* denotes the reaction constants of R1 and R2.

[b]. The HO_2 concentration is assumed to be with a magnitude of 10^8 molec cm^{-3} , which is consistent with Tan et al. (2018).

[c]. The production rates of R1 and R2 are calculated by $k[HO_2][NO]$ and $k[HO_2][HO_2]$, respectively.

Table S4. Comparisons of HCHO levels in recent studies in China with results in this study.

Location	Site type	Period	Conc. (ppb)	Reference
Beijing, China	Suburban NCP	Summer, 2008	11.17 ± 5.32	Yang et al. (2018)
Beijing, China	Suburban NCP	October, 2006	7.49	Pang et al. (2009)
Beijing, China	Urban NCP	Summer, 2013	11.4 ± 5.6	Rao et al. (2016)
		Winter, 2014	5.5 ± 3.9	
Beijing, China	Urban NCP	Summer, 2015	6.9 ± 2.9	Qian et al. (2019)
		Summer, 2018	8.5 ± 2.1	
		Winter, 2017	3.2 ± 2.4	
Beijing, China	Urban NCP	August, 2006	29.2 ± 12.1	Duan et al. (2012)
Beijing, China	Urban NCP	December, 2016	18.3 ± 7.2	Sheng et al. (2018)
Beijing, China	Suburban NCP	Autumn, 2005	15.8 ± 9.7	Zhang et al. (2012)
		Autumn, 2008	5.9 ± 3.2	
		Autumn, 2009	8.3 ± 5.8	
Beijing, China	Urban NCP	November, 2014	14.2 ± 13.8	Zhou et al. (2019)
		July, 2015	12.8 ± 4.8	
Wangdu, China	Rural NCP	Nov−Dec, 2017	3.7	Wang et al. (2020)
Shenzhen, Guangdong, China	Urban site	Spring, 2016	3.4 ±1.6	Wang et al. (2017)
		Summer, 2016	5.0 ± 4.4	
		Autumn, 2016	5.1 ± 3.1	
		Winter, 2016	4.2 ± 2.2	
Wujiasha, China	Suburban site	August, 2016	2.1 ± 0.2	Zeng et al. (2019b)
Ziyang, Sichuan, China	Urban site	August, 2016	2.2 ± 0.4	
Hankou, Hubei, China	Roadside site	August, 2016	3.4 ± 0.5	
Nanning, Guangxi, China	Urban site	Oct 2011−Jul 2012	5.6 ± 2.8	Guo et al. (2016)
Mount Tai, Shandong, China	Background site	Summer, 2014	3.5 ± 1.0	Yang et al. (2017)
Wuhan, Hubei, China	Suburban site	Feb, Apr, July, Oct of 2017	3.4 ± 2.0	Yang et al.(2019)
Guangzhou, Guangdong, China	Urban site	July, 2006	7.6 ± 3.7	Ling et al. (2017)
SDZ, Beijing, China	Rural site	Oct., 2020	4.6 ± 3.8	This study

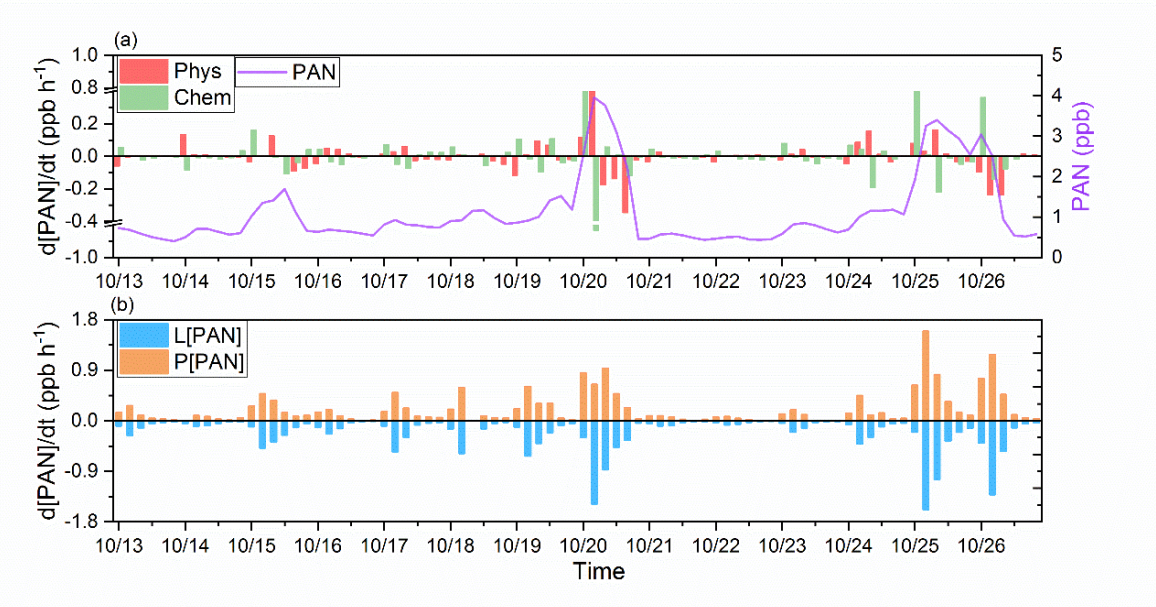

Figure S1. (a) Changes in PAN concentrations every four hours due to physical (Phys) and chemical (Chem) processes during the observation period at the SDZ site. (b) Chemical change rates of PAN due to chemical production (P[PAN]) and loss (L[PAN]) every four hours during the observation period at the SDZ site.